Collective Nuclear Excitation and Pulse Propagation in Single-Mode X-Ray Waveguides

Leon M. Lohse,[1,2,3,*] Petar Andrejić,[4] Sven Velten,[2,3] Malte Vassholz,[1] Charlotte Neuhaus,[1] Ankita Negi,[2,3] Anjali Panchwanee,[3] Ilya Sergeev,[3] Adriana Pálffy,[5] Tim Salditt,[1] and Ralf Röhlsberger[6,7,8,2,3]

[1]*Georg-August-Universität Göttingen, 37077 Göttingen, Germany*
[2]*The Hamburg Centre for Ultrafast Imaging, 22761 Hamburg, Germany*
[3]*Deutsches Elektronen-Synchrotron DESY, 22607 Hamburg, Germany*
[4]*Friedrich-Alexander-Universität Erlangen-Nürnberg, 91058 Erlangen, Germany*
[5]*Julius-Maximilians-Universität Würzburg, 97074 Würzburg, Germany*
[6]*Friedrich-Schiller-Universität Jena, 07743 Jena, Germany*
[7]*Helmholtz-Institut Jena, 07743 Jena, Germany*
[8]*GSI Helmholtzzentrum für Schwerionenforschung GmbH, 64291 Darmstadt, Germany*

(Received 2 March 2024; revised 16 April 2025; accepted 27 June 2025; published 30 July 2025)

Waveguides offer a means to controllably couple atomic ensembles to the electromagnetic field therein. Here, we demonstrate x-ray propagation in planar thin-film waveguides coupled to Mössbauer nuclei under collective resonant excitation by short pulses of synchrotron radiation. We record x-ray photons that have been emitted into resonant modes of the waveguide. Depending on the geometry and mode of excitation, two fundamentally different signatures of the collective emission are observed, for which we present a unifying theoretical model. Our results form a new platform for waveguide quantum electrodynamics in the hard x-ray regime with the potential to provide a coherent narrow band source of x-rays on the nanometer scale.

DOI: 10.1103/r2hf-9qn9

When interacting with radiation, ensembles of identical quantum optical systems exhibit collective dynamics, which is fundamentally different from that of the individual constituents [1]. Collective effects such as directed emission [2,3], collective frequency shifts, superradiant decay [4], and collective oscillations emerge already in the regime of weak excitation from as little as a single photon [5]. Furthermore, in spatially extended ensembles, the geometry and spatial distribution distinctively affects the dynamics [6,7]. These effects have been observed over various platforms, including one-dimensional chains of atoms coupled to optical waveguides [8–13] and Mössbauer nuclei in solid-state systems driven by hard x-rays [14–24]. The latter are a particularly well-suited platform to observe and harness collective effects, since nuclear transitions resonant to hard x-ray frequencies have extremely narrow linewidths [25], rendering exceptionally clean quantum optical systems [26,27], such that Mössbauer nuclei were among the earliest systems to investigate collective radiative phenomena (see Refs. [14,18,19,28] and the references therein).

*Contact author: llohse@uni-goettingen.de

The experimental platforms available so far for quantum optics with Mössbauer nuclei have been either nuclear forward scattering (NFS) from unstructured foils [20], nuclear Bragg diffraction (NBD) from crystals [14,15,17,24], or grazing-incidence reflection from thin-film structures [26]. Depending on the experimental geometry, the collective nuclear excitation—also known as nuclear exciton [14,18,19]—has a different temporal dynamics. In NFS, i.e., a thick slab or foil illuminated in normal incidence, the nuclear exciton exhibits so-called dynamical beats and emits into forward direction [20,29]. In contrast, a thin film embedded in an x-ray waveguide (WG) and excited in grazing-incidence illumination decays exponentially and emits into the direction of specular reflection—which we call reflection geometry—with superradiant speedup and a shifted resonance frequency compared to the single atom [22], similar to NBD [14,17,28]. Still unexplored is a waveguide geometry, where identical nuclei are coupled to photons that propagate confined in a waveguide. The waveguide allows some control over the modes of the photon field and their dispersion. Such systems have attracted a lot of attention recently in the emerging field of waveguide QED [30], yet so far restricted to longer photon wavelengths.

In this Letter, we demonstrate the excitation and collective dynamics of Mössbauer nuclei coupled in forward incidence to a single-mode nanometer-thin x-ray waveguide, resolved in both time and position. We present two experiments, in which we excite the sample either in

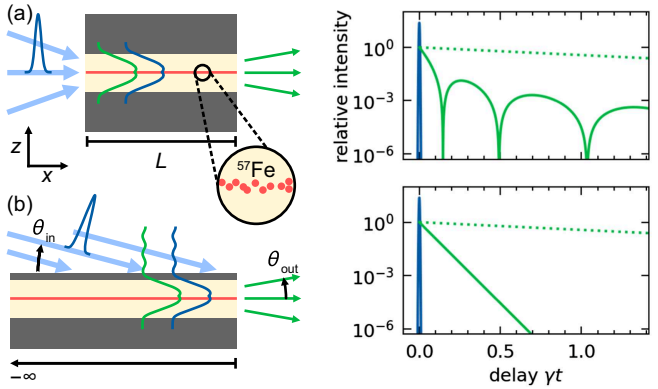

FIG. 1. A short excitation pulse (blue) couples into a planar WG and creates a nuclear exciton in the ^{57}Fe layer (red) that radiatively decays (green). (a) FC excitation creates an exciton that emits pronounced temporal beatings. (b) RBC excitation of a long WG: the exciton decays exponentially. Superradiant speedup and shifted resonance, compared to the natural exponential decay with rate γ (dotted green line), depend on the incidence angle θ_{in}. The plots on the right show exemplary theory calculations.

front-coupling (FC) geometry [Fig. 1(a)] [31] or resonant-beam-coupling (RBC) geometry [Fig. 1(b)] [32]. Our experimental technique combined with optimized WG designs and fabrication allows one to observe the photons that have been emitted into resonant modes of the WG leaving its back end. Depending on the way of excitation, the decay of the nuclear exciton either exhibits dynamical beats as in NFS or it decays exponentially with superradiant speedup. We explain our observations by a unifying theoretical model based on a recently introduced approach based on a real-space Green's function formalism [33]. Our results shed new light on earlier experiments in reflection geometry and open new ways to design spatiotemporal properties of the nuclear exciton based on hard x-ray waveguiding, thus benefiting the emerging field of waveguide QED [30].

Hard x-rays are an extreme regime for waveguiding. In the energy regime above 10 keV, refractive indices are written as $n = 1 - \delta + i\beta$, where $\delta, \beta < 10^{-5}$. X-ray waveguiding manifests when lighter core materials are surrounded by denser cladding materials. Because of the small contrasts in n, x-ray WGs are weakly guiding (modes typically extend over a few 100 wavelengths in the transversal direction) and cause significant photoelectric absorption in the dense cladding. Consequently, the Purcell enhancement is negligible and coupling to resonant modes is small [34]. However, dense cladding strongly attenuates everything but the lowest few resonant modes [35], so that fields generated by emitters in the WG can be asymptotically approximated by only their resonant components [34].

We have prepared two planar x-ray WGs, both containing a few-atomic-layers-thin iron film, to 95% enriched in ^{57}Fe, in the center of its guiding layer (see Supplemental Material [36]). The ^{57}Fe does not develop long-range magnetic order in this thin film and hence exhibits essentially a single resonance line. The experiments were performed at the dynamics beamline P01 at PETRA III (DESY, Hamburg) [41]. The samples were illuminated by 100-ps-long synchrotron pulses with photon energy 14.4 keV (monochromatized to 1 meV bandwidth) at a repetition period of 192 ns, creating nuclear excitons. The photons leaving the WG at its back end were detected with a stack of avalanche photo diodes (APDs). By temporal gating, the (delayed) emissions of the nuclear exciton are detected independent from the (prompt) synchrotron pulse.

First, we have prepared a layer system optimized for FC excitation, consisting of a 0.6-nm-thin layer of ^{57}Fe, embedded in a planar x-ray WG with 20 nm B_4C core, and symmetric 30-nm-thick Mo cladding as sketched in Fig. 2(a). The layer structure was deposited onto a 1-mm-thick Ge wafer and capped with a second Ge wafer after deposition, as detailed in Ref. [37]. The synchrotron beam was focused with two elliptical mirrors in Kirkpatrick-Baez geometry to a spot of about 7 μm diameter into the WG entrance at the focal position. The Ge wafers were used to

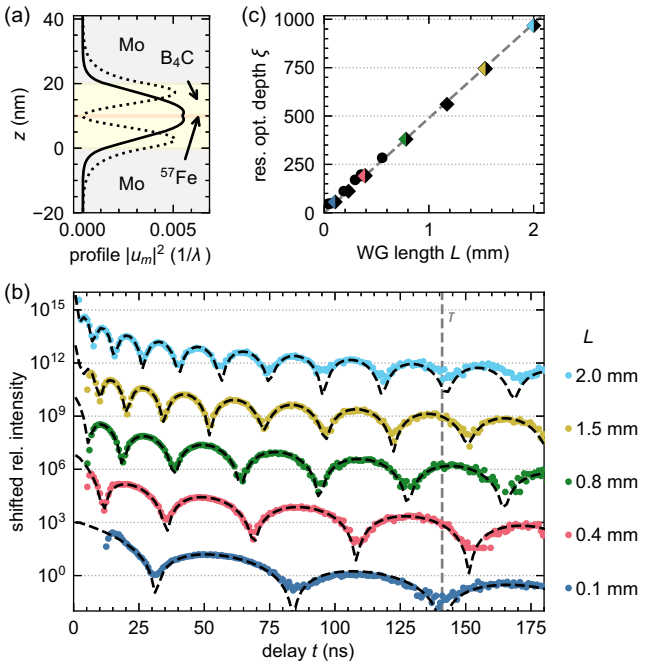

FIG. 2. Layer design and experimental data for FC excitation. (a) Transversal mode profiles $u_m(z)$ of the two guided modes supported by the WG. (b) Experimentally observed emissions as a function of delay t after excitation for different WG lengths L (colored points). The intensities are normalized and vertically shifted. The dashed lines show simulations of NFS through ^{57}Fe foils, using hyperfine parameters and resonant optical depth ξ that were estimated from the experimental data. (c) Extracted resonant optical depth ξ for different L (diamonds and disks indicate two independent measurements).

absorb the tails of the focus to reduce background signal, but they do not affect the resonant mode structure due to the thick cladding [42]. The wafer sandwich was cut to triangular shape, allowing us to change the effective WG length L by translating it along y transversal to the beam (see Supplemental Material [36]). The WG length was calibrated by measuring the absorption in the wafer as a function of y translation. Figure 2(b) shows the temporal evolution of the emitted x-rays for several WG lengths up to 2 mm (limited by off-resonant absorption). The emissions clearly exhibit dynamical beats resembling those known from NFS through a homogeneous single-line resonant absorber. The dashed lines show simulations of NFS through a thick foil of enriched ^{57}Fe including inhomogeneous hyperfine splitting in the order of six natural linewidths, in a four-parameter model (see Supplemental Material [36]), which accurately describes the data. The optimal parameters were found using a maximum-likelihood estimation assuming Poisson statistics. The magnitude of hyperfine splitting is expected from similar amorphous thin films [22,43]. The extracted optical depth ξ (also called "effective thickness" [20]) [Fig. 2(c)] is strictly proportional to the WG length L.

For the second experiment, we have prepared a layer system optimized for RBC excitation [Fig. 1(b)], having a 40-nm-thick B_4C core and, in contrast to the FC experiment, a top Mo cladding layer of only 8 nm to allow incident light to evanescently couple into the WG. We used a 10-mm-long Si wafer as substrate, so that the WG is significantly longer than the attenuation length of the resonant modes and thus has effectively infinite extent. The back end of the sample was broken off after deposition to create a clean exit face. The sample was placed onto a goniometer stage for tuning the incidence angle θ_{in}. Figure 3 shows the off-resonant far-field intensity distribution, detected 3 m downstream of the sample by a time-insensitive pixel detector as a function of θ_{in}. We then aligned the APDs with the WG exit [$\theta_{out} \approx 0°$, see Fig. 1(b)] and collected the emitted photons for several values of θ_{in} in the vicinity of the third resonance $\theta_3 = 0.203°$. We selected the third mode for practical reasons, because the divergence of the incident beam was 0.002°, which is wider than the resonance of the first mode. Figure 4(a) shows the emitted intensity as a function of time for three different θ_{in}. The intensity exhibits an initial superradiant decay and a slowdown for longer delays, which is caused by a residual hyperfine splitting of the nuclear levels. The initial decay is plotted in Fig. 4(b), showing a decay rate of 30γ at θ_3, which gradually diminishes as θ_{in} moves away from resonance. Similar behavior was previously observed with NBD [17] and thin films in reflection geometry [22]. The solid line shows a simulation in reflection geometry [36] that considers divergence of the incoming beam and hyperfine splitting of the transitions. The hyperfine parameters for the simulation were extracted from measurements at $\theta_{in} = 0.5°$, far from the WG modes, and are consistent with the FC experiment [36].

To qualitatively model the experimental observations, we employ the theory developed in Ref. [33] based on macroscopic quantum electrodynamics, which describes the atom-light interaction using the classical electromagnetic Green's function. Importantly, it explicitly models the propagating field modes in the dispersive waveguide environment with spatial dependency, which has not been relevant for the existing theories of NFS [29,44], NBD [18,28], or the reflection geometry [45–47]. Here, we neglect the nearly degenerate sublevels of the ground

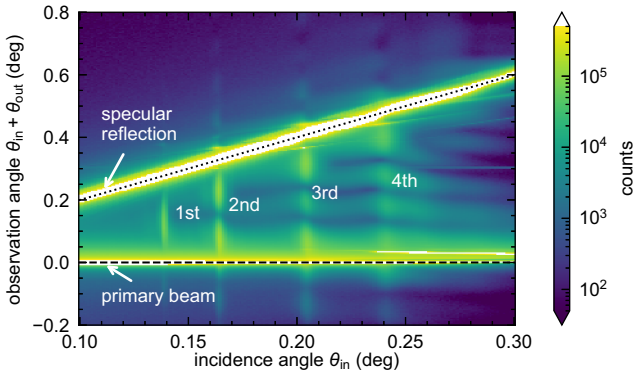

FIG. 3. Off-resonant intensity of the RBC sample, illuminated at an incidence angle of θ_{in} and recorded 3 m downstream of the sample with a pixel detector. Vertical cuts correspond to observed far-field patterns. The four resonant modes, which are supported by the layer structure, are clearly visible in the region between the primary beam ($\theta_{in} + \theta_{out} = 0$) and the specularly reflected beam ($\theta_{out} = \theta_{in}$). The modes are well separated in θ_{in}.

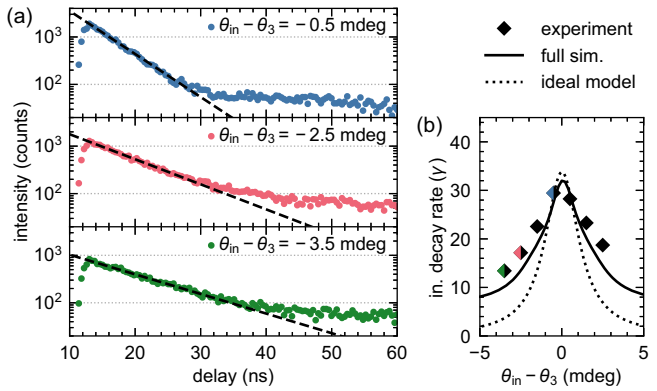

FIG. 4. Experimentally measured emissions of the nuclear exciton in RBC excitation. (a) Decay pattern for three angles in the vicinity of the third resonant mode and initial exponential decay (black dashed line). (b) Initial decay rate as a function of angle detuning: extracted from the experimental data (black diamonds); calculated with the simplified ideal model (7) (dashed line); simulation including hyperfine splitting of the transition energies as well as the angular divergence of the experiment (solid line).

($I_g = 1/2$) and excited ($I_e = 3/2$) state of ^{57}Fe ($\hbar\omega_0 = 14.4$ keV, $\hbar\gamma = 4.7$ neV, $M1$ transition) and describe the nuclear state by a single nuclear transition operator for each atom $\hat{\sigma}^i_{ge} = |g\rangle\langle e|$. The excitation pulses have very small pulse areas so that the nuclear excited states remain unpopulated ($\langle\hat{\sigma}^i_{ee}\rangle \approx 0$) and the response is linear. The expectation values of the transition operators $\sigma^i_{ge} := \langle\hat{\sigma}^i_{ge}\rangle$ evolve, in the rotating frame of the nuclear transition frequency ω_0, according to [8]

$$-i\omega\sigma^i_{ge}(\omega) = -\frac{\gamma}{2}\sigma^i_{ge}(\omega) + i\Omega(\mathbf{r}_i,\omega) + i\sum_{j\neq i} g_{ij}(\omega)\sigma^j_{ge}(\omega), \tag{1}$$

where $\Omega(\mathbf{r},t) = \mathbf{m}_0^* \cdot \mathbf{B}_{\text{in}}(\mathbf{r},t)/\hbar$ is the propagating excitation pulse expressed as a Rabi frequency, $\mathbf{m}_0$ is the magnetic dipole moment of the transition, and g_{ij} are dispersive coupling coefficients. The total single-atom spontaneous decay rate γ includes self-interaction and is equal to its value in a homogeneous environment (negligible Purcell factor). Note that $\mathbf{B}_{\text{in}}$ is the free incident magnetic field and scattering from the nuclei is fully accounted for by g_{ij}. The coupling is mediated by the WG environment via

$$g_{ij}(\omega) := \frac{\mu_0 k_0^2}{\hbar}\mathbf{m}_0^* \cdot \overleftrightarrow{\mathrm{G}}_{\mathrm{m}}(\mathbf{r}_i,\mathbf{r}_j,\omega_0+\omega)\cdot\mathbf{m}_0, \tag{2}$$

where μ_0 is the vacuum permeability, $k_0 = \omega_0/c$, and $\overleftrightarrow{\mathrm{G}}_{\mathrm{m}}$ is the Green's function for the magnetic field in the WG (see Supplemental Material [36]). While the σ^i_{ge} are defined in the rotating frame, this Green's function depends on the absolute frequency $\omega_0 + \omega$.

We convert (1) into a one-dimensional macroscopic equation. To that end, we assume homogeneously distributed nuclei in a single thin layer, insert the analytic expression for the Green's function, and assume interaction via a single resonant mode. We obtain

$$\dot{\sigma}_{ge}(x,t) = -\frac{\gamma}{2}\sigma_{ge}(x,t) + i\Omega(x,t) - \frac{\zeta_m\gamma}{4\Lambda_{\text{res}}} \times \int_{-L}^{0} \mathrm{d}x' e^{ik_0\nu_m|x-x'|}\sigma_{ge}(x', t-|x-x'|\nu_m/c). \tag{3}$$

Here, Λ_{res} is the on-resonance attenuation length (61 nm for bulk ^{57}Fe), ν_m is the complex effective refractive index of the mode [34], and ζ_m is the dimensionless coupling coefficient of the WG mode. The latter effectively rescales Λ_{res} and is given by $\zeta_m = d u_m(z_0)^2$, where d and z_0 are thickness and position of the ^{57}Fe layer, respectively, and $u_m(z)$ is the complex transversal mode profile, described in Ref. [34], which is binormalized to $\int[u_m(z)]^2\mathrm{d}z = 1$. The field radiated by the nuclear exciton is obtained via

$$\mathbf{B}^+_{\text{nuc}}(\mathbf{r},\omega) = \mu_0 k_0^2 \sum_j \overleftrightarrow{\mathrm{G}}_{\mathrm{m}}(\mathbf{r},\mathbf{r}_j,\omega_0+\omega)\cdot\mathbf{m}_0\sigma^j_{ge}(\omega), \tag{4}$$

corresponding to the field radiated by the oscillating magnetization $\mathbf{M} = \mathbf{m}_0\rho\sigma_{ge}\exp(-i\omega_0 t) + \text{H.c.}$ Note that (3) not only describes planar WGs (after integrating out y) as discussed here, but also one-dimensional channel WGs and, furthermore, homogeneous slabs (foils) with translational symmetry in y-z [48], with different values for ν_m ($= n$ for slab) and ζ_m ($= 1$ for slab).

Equation (1) is often treated as an eigenvalue problem, decomposing σ_{ge} into radiative eigenmodes [6–8]. Instead, we employ a forward-scattering approximation that allows us to solve (3) analytically for the two experimental settings sketched in Fig. 1. The rapidly oscillating phase factor in (3) strongly suppresses the backscattered field [33]. Hence, we change the upper limit of integration in (3) to x.

In the FC geometry [Fig. 1(a)], the only surviving component of the excitation pulse is the fundamental guided mode, so that $\Omega(x,t) = \Omega_0\exp(ik_0\nu_m x)\Pi(t_{\text{ret}})$, with some slowly varying envelope $\Pi(t)$ where $t_{\text{ret}} = t - k_0\nu_m x/c$. Note that the excitation pulse decays with x, as $\text{Im}\{\nu_m\} > 0$. For finite L, (3) becomes a Volterra integral equation due to the forward-scattering approximation and hence has no radiative eigenmodes. Its exact analytical solution for the given $\Omega(x,t)$ is

$$\sigma_{ge}(x,t) = iAe^{ik_0\nu_m x - \gamma t_{\text{ret}}/2} J_0\left[\sqrt{\gamma t_{\text{ret}} x\zeta_m\Lambda_{\text{res}}^{-1}}\right], \tag{5}$$

for $t_{\text{ret}} \geq 0$, where J_0 is a Bessel function of the first kind and $A = \Omega_0\int\Pi(t)\mathrm{d}t$ is the pulse area. This is the well-known solution for NFS [29,44] with Λ_{res} rescaled by ζ_m. Computing the emitted field from (5) is straightforward (see Supplemental Material [36]). The exciton emits directionally and purely into the WG mode. The emission undergoes the dynamical beats, well known from coherent pulse propagation through resonant media [20,28]—and clearly observed in our experiment. From the experimental data, we obtain an estimate for the coupling coefficient $|\zeta_m| = \xi\Lambda_{\text{res}}/L \approx 0.030$. The theoretical value (from design parameters) of 0.038 is slightly greater, likely because the number of iron atoms in the waveguide was less than designed.

In the RBC geometry [Fig. 1(b)], the incidence angle θ_{in} fixes the in-plane wave vector to $k_{\text{in}} = k_0\cos\theta_{\text{in}}$. The excitation pulse can be written as $\Omega(x,t) = \Omega_0\exp(ik_{\text{in}}x)\Pi(t_{\text{ret}})$, with here $t_{\text{ret}} = t - k_{\text{in}}x/\omega_0$. Assuming that L is significantly larger than the off-resonance attenuation length of the mode, $\Lambda_m = (2k_0\,\text{Im}\{\nu_m\})^{-1}$ (typically a few 100 μm), we can extend the lower boundary of integration in (3) to $-\infty$. This eliminates the boundary effect in the forward direction. The linear spatial phase in $\Omega(x,t)$ corresponds to a radiative eigenmode of the exciton, so that the exciton evolves

harmonically with shifted frequency and enhanced decay. We obtain (see Supplemental Material [36])

$$\sigma_{ge}(x,t) = iA \exp\left[ik_0 x \cos\theta_{\text{in}} - \left(\frac{\gamma}{2} - i\eta\right)t_{\text{ret}}\right], \quad (6)$$

$$\eta(\theta_{\text{in}}) = \frac{\zeta_m \Lambda_m}{\Lambda_{\text{res}}} \frac{1}{2\Lambda_m q_\theta - i}\frac{\gamma}{2}, \quad (7)$$

with $q_\theta = k_0 \cos\theta_{\text{in}} - k_0 \text{Re}\{\nu_m\} \approx -k_0(\theta_{\text{in}} - \theta_m)\sin\theta_m$ and pulse area A as previously defined. The mode angle is defined via $\cos\theta_m = \text{Re}\{\nu_m\}$. Similar to NBD [17,28], the exciton decays superradiantly with peak speedup of $1 + \zeta_m \Lambda_m/\Lambda_{\text{res}}$ depending on the ratio between off- and on-resonant attenuation lengths, as well as the mode coupling coefficient ζ_m. Note that $\Lambda_m/\Lambda_{\text{res}} = \rho\Lambda_m\sigma_{\text{res}}$ (σ_{res}, resonant cross section; ρ, number density of nuclei) gives the number of nuclei within the off-resonant absorption length (compare Ref. [27]), clearly demonstrating the collective superradiant nature of the speedup, contrasting earlier interpretations based on an increase of the photon density of states [21]. Figure 4(b) shows the speedup from calculations (dashed line) with (7) using the design parameters as well as the speedup from the experimental data (diamonds). This simple single-mode model already explains the observed peak speedup. It does not fully account for the increased angular resonance width, which can be attributed to the residual hyperfine splitting and angular divergence observed in the experiment [36]. Thus, we see that (3) qualitatively reproduces both experiments. Notably, similar eigenmodes (6) are observed in crystals [17] and waveguides in grazing-incidence reflection geometry [26].

In summary, we have demonstrated the excitation and collective dynamics of Mössbauer nuclei in x-ray waveguides for two different modes of excitation. In the FC geometry, we have observed dynamical beats emitted by WGs with a 20-nm-thick guiding core and varying lengths from about 0.1 to 2 mm into the fundamental WG mode. In the RBC geometry, we have observed exponential decay into the resonantly excited WG mode with tunable superradiant speedup. Our theory consistently describes the observations of both experiments in a one-dimensional waveguide picture. When a single mode dominates, the equation of motion is formally identical to that of a homogeneous slab with length (thickness) rescaled by a nucleus-mode coupling constant ζ_m. Depending on the off-resonant optical thickness of the WG, two regimes are realized. For optically thin WGs, the finite integrated nuclear density gives rise to dynamical beats. The grazing-incidence geometry allows the study of optically thick WGs, where off-resonant absorption suppresses boundary effects, establishing translation invariance and permitting radiative eigenmodes, so that the exciton evolves harmonically with resonant dispersion relation.

Our results open up a number of promising future directions. We demonstrated how to "harvest" the propagating beam at the exit of the WG, forming an extremely coherent narrow band source of 20 nm cross section, albeit with low brightness. Both the spatial diffraction patterns and temporal dynamics can be readily resolved at these scales. The FC geometry allows one to simultaneously and coherently couple into multiple guided modes in one or several WGs. A multimode WG could be used to implement effective two-beam control techniques for the x-ray frequency regime. The spatial coherence allows one to spatially separate individual modes and permits new approaches for narrow band x-ray control via the engineering of collective radiation patterns. The source may be utilized for investigations at the nanoscale that leverage both spatial and temporal coherence.

Acknowledgments—We thank Mike Kanbach for preparing the WG assemblies, Olaf Leupold for his support and fruitful discussions during the first beam time, and Dieter Lott and Helmholtz-Zentrum Hereon for providing and supporting the reflectometer to calibrate the thin-film samples. We acknowledge DESY (Hamburg, Germany), a member of the Helmholtz Association HGF, for the provision of experimental facilities. Beam time was allocated for Proposals No. I-20211677 and No. I-20221193. We acknowledge partial funding by Max Planck School of Photonics; Deutsche Forschungsgemeinschaft (DFG) (432680300 SFB 1456/C03, 429529648 TRR 306/C04, 390858490 EXC 2147, 390715994 EXC 2056). A. Pálffy acknowledges support from the DFG in the framework of the Heisenberg Program.

Data availability—The data that support the findings of this Letter are openly available [49].

[1] R. H. Dicke, Coherence in spontaneous radiation processes, Phys. Rev. **93**, 99 (1954).
[2] M. O. Scully, E. S. Fry, C. H. Raymond Ooi, and K. Wódkiewicz, Directed spontaneous emission from an extended ensemble of N atoms: Timing is everything, Phys. Rev. Lett. **96**, 010501 (2006).
[3] J. H. Eberly, Emission of one photon in an electric dipole transition of one among N atoms, J. Phys. B **39**, S599 (2006).
[4] M. O. Scully, Collective Lamb shift in single photon Dicke superradiance, Phys. Rev. Lett. **102**, 143601 (2009).
[5] M. O. Scully and A. A. Svidzinsky, The super of superradiance, Science **325**, 1510 (2009).
[6] A. A. Svidzinsky, J.-T. Chang, and M. O. Scully, Cooperative spontaneous emission of N atoms: Many-body eigenstates, the effect of virtual Lamb shift processes, and analogy with radiation of N classical oscillators, Phys. Rev. A **81**, 053821 (2010).

[7] J. T. Manassah, Cooperative radiation from atoms in different geometries: Decay rate and frequency shift, Adv. Opt. Photonics **4**, 108 (2012).

[8] A. Asenjo-Garcia, J. D. Hood, D. E. Chang, and H. J. Kimble, Atom-light interactions in quasi-one-dimensional nanostructures: A Green's-function perspective, Phys. Rev. A **95**, 033818 (2017).

[9] P. Solano, P. Barberis-Blostein, F. K. Fatemi, L. A. Orozco, and S. L. Rolston, Super-radiance reveals infinite-range dipole interactions through a nanofiber, Nat. Commun. **8**, 1857 (2017).

[10] J. Kumlin, K. Kleinbeck, N. Stiesdal, H. Busche, S. Hofferberth, and H. P. Büchler, Nonexponential decay of a collective excitation in an atomic ensemble coupled to a one-dimensional waveguide, Phys. Rev. A **102**, 063703 (2020).

[11] R. Pennetta, M. Blaha, A. Johnson, D. Lechner, P. Schneeweiss, J. Volz, and A. Rauschenbeutel, Collective radiative dynamics of an ensemble of cold atoms coupled to an optical waveguide, Phys. Rev. Lett. **128**, 073601 (2022).

[12] S. Cardenas-Lopez, P. Solano, L. A. Orozco, and A. Asenjo-Garcia, Optical precursors in waveguide quantum electrodynamics, Phys. Rev. Res. **5**, 013133 (2023).

[13] D. Su, Y. Jiang, S. Cardenas-Lopez, A. Asenjo-Garcia, P. Solano, L. A. Orozco, and Y. Zhao, Dynamical beats of short pulses in waveguide QED, Phys. Rev. Res. **5**, L042041 (2023).

[14] A. M. Afanas'ev and Y. Kagan, Radiation of a system of excited nuclei in a crystal, JETP Lett. **2**, 130 (1965).

[15] E. Gerdau, R. Rüffer, H. Winkler, W. Tolksdorf, C. P. Klages, and J. P. Hannon, Nuclear Bragg diffraction of synchrotron radiation in yttrium iron garnet, Phys. Rev. Lett. **54**, 835 (1985).

[16] U. van Bürck, R. L. Mössbauer, E. Gerdau, R. Rüffer, R. Hollatz, G. V. Smirnov, and J. P. Hannon, Nuclear Bragg scattering of synchrotron radiation with strong speedup of coherent decay, measured on antiferromagnetic $^{57}FeBO_3$, Phys. Rev. Lett. **59**, 355 (1987).

[17] Y. V. Shvyd'ko and G. V. Smirnov, Experimental study of time and frequency properties of collective nuclear excitations in a single crystal (gamma-ray resonance), J. Phys. Condens. Matter **1**, 10563 (1989).

[18] J. P. Hannon and G. T. Trammell, Coherent γ-ray optics, Hyperfine Interact. **123–124**, 127 (1999).

[19] G. V. Smirnov, General properties of nuclear resonant scattering, Hyperfine Interact. **123–124**, 31 (1999).

[20] U. van Bürck, Coherent pulse propagation through resonant media, Hyperfine Interact. **123–124**, 483 (1999).

[21] R. Röhlsberger, K. Schlage, T. Klein, and O. Leupold, Accelerating the spontaneous emission of x rays from atoms in a cavity, Phys. Rev. Lett. **95**, 097601 (2005).

[22] R. Röhlsberger, K. Schlage, B. Sahoo, S. Couet, and R. Rüffer, Collective Lamb shift in single-photon superradiance, Science **328**, 1248 (2010).

[23] J. Haber, X. Kong, C. Strohm, S. Willing, J. Gollwitzer, L. Bocklage, R. Rüffer, A. Pálffy, and R. Röhlsberger, Rabi oscillations of x-ray radiation between two nuclear ensembles, Nat. Photonics **11**, 720 (2017).

[24] A. I. Chumakov, A. Q. R. Baron, I. Sergueev, C. Strohm, O. Leupold, Y. Shvyd'ko, G. V. Smirnov, R. Rüffer, Y. Inubushi, M. Yabashi, K. Tono, T. Kudo, and T. Ishikawa, Superradiance of an ensemble of nuclei excited by a free electron laser, Nat. Phys. **14**, 261 (2017).

[25] R. Röhlsberger, Nuclear Condensed Matter Physics with Synchrotron Radiation, *Springer Tracts in Modern Physics* (Springer, Berlin; Heidelberg, 2005).

[26] R. Röhlsberger and J. Evers, Quantum optical phenomena in nuclear resonant scattering, in *Modern Mössbauer Spectroscopy*, Topics in Applied Physics, edited by Y. Yoshida and G. Langouche (Springer, Singapore, 2021), pp. 105–171.

[27] B. W. Adams, Nuclear γ-ray superradiance, J. Mod. Opt. **56**, 1974 (2009).

[28] Y. Kagan, A. M. Afanas'ev, and V. G. Kohn, On excitation of isomeric nuclear states in a crystal by synchrotron radiation, J. Phys. C **12**, 615 (1979).

[29] G. V. Smirnov, U. van Bürck, J. Arthur, G. S. Brown, A. I. Chumakov, A. Q. R. Baron, W. Petry, and S. L. Ruby, Currents and fields reveal the propagation of nuclear polaritons through a resonant target, Phys. Rev. A **76**, 043811 (2007).

[30] A. S. Sheremet, M. I. Petrov, I. V. Iorsh, A. V. Poshakinskiy, and A. N. Poddubny, Waveguide quantum electrodynamics: Collective radiance and photon-photon correlations, Rev. Mod. Phys. **95**, 015002 (2023).

[31] C. Fuhse, A. Jarre, C. Ollinger, J. Seeger, T. Salditt, and R. Tucoulou, Front-coupling of a prefocused x-ray beam into a monomodal planar waveguide, Appl. Phys. Lett. **85**, 1907 (2004).

[32] Y. P. Feng, S. K. Sinha, H. W. Deckman, J. B. Hastings, and D. P. Siddons, X-ray flux enhancement in thin-film waveguides using resonant beam couplers, Phys. Rev. Lett. **71**, 537 (1993).

[33] P. Andrejić, L. M. Lohse, and A. Pálffy, Waveguide QED with Mössbauer nuclei, Phys. Rev. A **109**, 063702 (2024).

[34] L. M. Lohse and P. Andrejić, Nano-optical theory of planar x-ray waveguides, Opt. Express **32**, 9518 (2024).

[35] M. Osterhoff and T. Salditt, Coherence filtering of x-ray waveguides: Analytical and numerical approach, New J. Phys. **13**, 103026 (2011).

[36] See Supplemental Material at http://link.aps.org/supplemental/10.1103/r2hf-9qn9, which includes Refs. [33–35,37–40], for more information on the theoretical model, sample design, experimental setup, and data analysis.

[37] S. P. Krüger, H. Neubauer, M. Bartels, S. Kalbfleisch, K. Giewekemeyer, P. J. Wilbrandt, M. Sprung, and T. Salditt, Sub-10 nm beam confinement by x-ray waveguides: Design, fabrication and characterization of optical properties, J. Synchrotron Radiat. **19**, 227 (2012).

[38] T. Gruner and D.-G. Welsch, Green-function approach to the radiation-field quantization for homogeneous and inhomogeneous Kramers-Kronig dielectrics, Phys. Rev. A **53**, 1818 (1996).

[39] R. Röhlsberger, Theory of x-ray grazing incidence reflection in the presence of nuclear resonance excitation, Hyperfine Interact. **123–124**, 301 (1999).

[40] L. Bocklage, Nexus - Nuclear Elastic X-ray scattering Universal Software (v1.2.0), Zenodo (2024), 10.5281/zenodo.13832946.

[41] H.-C. Wille, H. Franz, R. Röhlsberger, W. A. Caliebe, and F.-U. Dill, Nuclear resonant scattering at PETRA III: Brillant opportunities for nano—and extreme condition science, J. Phys. Conf. Ser. **217**, 012008 (2010).

[42] T. Salditt, S. P. Krüger, C. Fuhse, and C. Bähtz, High-transmission planar x-ray waveguides, Phys. Rev. Lett. **100**, 184801 (2008).

[43] B. Sahoo, K. Schlage, J. Major, U. von Hörsten, W. Keune, H. Wende, and R. Röhlsberger, Preparation and characterization of ultrathin stainless steel films, in *AIP Conference Proceedings* (AIP, New York, 2011), Vol. 1347.

[44] Y. V. Shvyd'ko, Nuclear resonant forward scattering of x rays: Time and space picture, Phys. Rev. B **59**, 9132 (1999).

[45] K. P. Heeg and J. Evers, X-ray quantum optics with Mössbauer nuclei embedded in thin-film cavities, Phys. Rev. A **88**, 043828 (2013).

[46] D. Lentrodt, K. P. Heeg, C. H. Keitel, and J. Evers, Ab initio quantum models for thin-film x-ray cavity QED, Phys. Rev. Res. **2**, 023396 (2020).

[47] D. Lentrodt, O. Diekmann, C. H. Keitel, S. Rotter, and J. Evers, Certifying multimode light-matter interaction in lossy resonators, Phys. Rev. Lett. **130**, 263602 (2023).

[48] R. Friedberg and J. T. Manassah, Eigenfunctions and eigenvalues in superradiance with x-y translational symmetry, Phys. Lett. A **372**, 2787 (2008).

[49] L. M. Lohse, S. Velten, C. Neuhaus, A. Negi, A. Panchwanee, I. Sergeev, T. Salditt, and R. Röhlsberger, Experimental Data for: Collective nuclear excitation and pulse propagation in single-mode x-ray waveguides, GRO.-data V2 (2025), 10.25625/F8CRVT.